

Empirical priors for prediction in sparse high-dimensional linear regression

Ryan Martin* and Yiqi Tang*

December 15, 2024

Abstract

Often the primary goal of fitting a regression model is prediction, but the majority of work in recent years focuses on inference tasks, such as estimation and feature selection. In this paper we adopt the familiar sparse, high-dimensional linear regression model but focus on the task of prediction. In particular, we consider a new empirical Bayes framework that uses the data to appropriately center the prior distribution for the non-zero regression coefficients, and we investigate the method's theoretical and numerical performance in the context of prediction. We show that, in certain settings, the asymptotic posterior concentration in metrics relevant to prediction quality is very fast, and we establish a Bernstein–von Mises theorem which ensures that the derived prediction intervals achieve the target coverage probability. Numerical results complement the asymptotic theory, showing that, in addition to having strong finite-sample performance in terms of prediction accuracy and uncertainty quantification, the computation time is considerably faster compared to existing Bayesian methods.

Keywords and phrases: Bayesian inference; data-dependent prior; model averaging; predictive distribution; uncertainty quantification.

1 Introduction

Consider a linear regression model

$$y = X\beta + \sigma z,$$

where y is a $n \times 1$ vector of response variables, X is a $n \times p$ matrix of explanatory variables, β is a $p \times 1$ vector of regression parameters, $\sigma > 0$ is an unknown scale parameter, and z is a $n \times 1$ vector of independent standard normal errors. Here, our interest is in the high-dimensional setting where $p \gg n$, and our particular aim is to predict the value of a new response $\tilde{y} \in \mathbb{R}^d$ at a given $\tilde{X} \in \mathbb{R}^{d \times p}$, $d \geq 1$, an important and challenging problem in these high-dimensional scenarios.

*Department of Statistics, North Carolina State University, 2311 Stinson Dr., Raleigh, NC 27695.
Email: rgmarti3@ncsu.edu, ytang22@ncsu.edu

An initial obstacle to achieving this aim is that the model above cannot be fit without some additional structure. As is common in the literature, we will assume a sparsity structure on the high-dimensional β vector. That is, we will assume that most of the entries in β are zero; this will be made more precise in the following sections. With this assumed structure, a plethora of methods are now available for estimating a sparse β , e.g., lasso (Tibshirani 1996), adaptive lasso (Zou 2006), SCAD (Fan and Li 2001), and others; moreover, software is available to carry out the relevant computations easily and efficiently. Given an estimator of β , it is conceptually straightforward to produce a point prediction of a new response. However, the regularization techniques employed by these methods cause the estimators to have non-regular distribution theory (e.g., Pötscher and Leeb 2009), so results on uncertainty quantification, i.e., coverage properties of prediction intervals, are few in number; but see Leeb (2006, 2009) and the references therein.

On the Bayesian side, given a full probability model, it is conceptually straightforward to obtain a predictive distribution for the new response and suggest some form of uncertainty quantification, but there are still a number of challenges. First, in high-dimensional cases such as this, the choice of prior matters, so specifying prior distributions that lead to desirable operating characteristics of the posterior distribution, e.g., optimal posterior concentration rates, is non-trivial. Castillo et al. (2015) and others have demonstrated that in order to achieve the optimal concentration rates, the prior for the non-zero β coefficients must have sufficiently heavy tails, in particular, heavier than the conjugate Gaussian tails. This constraint leads to the second challenge, namely, computation of the posterior distribution. While general Markov chain Monte Carlo (MCMC) methods are available, the individual steps can be expensive and the chain can be slow to converge. Some believe these computations to be prohibitively slow for priors that include a discrete component for the zero coefficients, so they prefer continuous shrinkage priors like the horseshoe (Carvalho et al. 2010) and Dirichlet–Laplace (Bhattacharya et al. 2015). In any case, even if the first two challenges can be overcome and a predictive distribution for \tilde{y} can be obtained, it is not automatic that the prediction intervals from this distribution provide valid uncertainty quantification, i.e., that the posterior 95% predictive interval will contain the to-be-observed value of \tilde{y} with probability 0.95.

The computational difficulties mentioned above stem from the need to work with the heavy-tailed priors that yield desired posterior concentration properties. Inspired by the insight that prior tails would be irrelevant if the prior center was appropriately chosen, Martin et al. (2017) developed an approach based on *empirical* or *data-dependent* priors in this high-dimensional regression setting. Their approach is powerful because it allows for conjugate priors to be used, which drastically speeds up computation, but without sacrificing on the desirable concentration rate properties enjoyed by the fully Bayesian approach with heavy-tailed priors.

Our goal in the present paper is to investigate the performance of the empirical Bayes approach in Martin et al. (2017) in the context of predicting a new response. After a review of their empirical Bayes formulation in Section 2, we focus on the computational and theoretical properties of the corresponding predictive distribution in Section 3. In particular, thanks to the empirical prior’s conjugacy, the corresponding predictive distribution has a very simple form and can be easily and efficiently sampled via standard Monte Carlo techniques. Moreover, we show that the same predictive distribution has fast convergence rates, nearly parametric in some cases, and that under reasonable as-

sumptions, a Bernstein–von Mises theorem holds, which implies that the derived posterior prediction intervals have the target coverage probability asymptotically. In Section 4 we demonstrate, in both real- and simulated-data examples, that the proposed empirical Bayes framework provides accurate point prediction, valid prediction uncertainty quantification, and fast computation across various settings compared to a number of existing methods. Finally, some concluding remarks are given in Section 5.

2 Empirical prior for regression

2.1 Known σ^2

Here we review the empirical prior approach for sparse, high-dimensional regression laid out in Martin et al. (2017). Like Castillo et al. (2015) and others, they focus on the known- σ^2 case, so we present their formulation here. Adjustments to handle the more realistic unknown- σ^2 case are described in Section 2.2.

Under the sparsity assumption, it is natural to decompose the high-dimensional vector β as (S, β_S) , where $S \subseteq \{1, 2, \dots, p\}$ is the configuration of β , i.e., the set of indices corresponding to non-zero/active coefficients, and β_S is the $|S|$ -vector of non-zero values; here $|S|$ denotes the cardinality of the finite set S . This decomposition suggests a hierarchical model with a marginal prior for S and a conditional prior for β_S , given S .

For the marginal prior for S , we take the mass function

$$\pi(S) = \binom{p}{|S|}^{-1} q_n(|S|), \quad S \subset \{1, 2, \dots, p\}, \quad |S| \leq R, \quad (1)$$

where q_n is a mass function on $\{0, 1, \dots, R\}$, which we take to be

$$q_n(s) \propto (cp^a)^{-s}, \quad s = 0, 1, \dots, R, \quad (2)$$

with $R = \text{rank}(X)$ and (a, c) some hyperparameters to be specified; see Section 4. This corresponds to a truncated geometric prior on the configuration size and a uniform prior on all configurations of the given size; see, also, Castillo et al. (2015). There is an assumption hidden in the definition (1) that deserves comment. The prior does not support all possible configurations, only those of size no more than $R \leq n \ll p$. The rationale for this restriction is that β is assumed to be sparse in the sense that the true configuration is of size much smaller than n , so there is no serious reason for not incorporating that assumption into the prior.

The empirical or data-dependent element comes in the conditional prior for β_S , given S . That is, set

$$\beta_S \mid S \sim \mathbf{N}_{|S|}(\hat{\beta}_S, \sigma^2 \gamma^{-1} (X_S^\top X_S)^{-1}),$$

where X_S is the $n \times |S|$ submatrix of X with only the columns corresponding to the configuration S , $\hat{\beta}_S$ is the least squares estimate based on design matrix X_S , and $\gamma > 0$ is a precision parameter to be specified. Except for being centered on the least squares estimator, this closely resembles the familiar Zellner’s g -prior (e.g., Zellner 1986). Again, the idea behind a data-dependent centering is to remove the influence of the prior tails on the posterior concentration, which requires use of the data. See Martin and Walker (2014, 2017) and Martin et al. (2017) for more on this point.

Putting the two pieces together, we have the following empirical prior for β :

$$\Pi_n(d\beta) = \sum_S \pi(S) \mathbf{N}_{|S|}(d\beta_S \mid \hat{\beta}_S, \sigma^2 \gamma^{-1} (X_S^\top X_S)^{-1}) \otimes \delta_{0_{S^c}}(d\beta_{S^c}), \quad (3)$$

where $\delta_{0_{S^c}}$ denotes a Dirac point-mass distribution at the origin in the $|S^c|$ -dimensional space, and $\mu \otimes \nu$ is the product of two measures μ and ν . This is a spike-and-slab prior where the spikes are point masses and the slabs are conjugate normal densities, which have nice computational properties but are centered at a convenient estimator to eliminate the thin-tail effect on the posterior concentration rate.

Next we combine this prior with the likelihood in almost the usual way. That is, for a constant $\alpha \in (0, 1)$, define the corresponding empirical Bayes posterior Π^n for β as

$$\Pi^n(d\beta) \propto L_n(\beta)^\alpha \Pi_n(d\beta),$$

where

$$L_n(\beta) = \mathbf{N}_n(y \mid X\beta, \sigma^2 I) \propto \exp\{-\frac{1}{2\sigma^2} \|y - X\beta\|^2\}, \quad (4)$$

is the likelihood, with $\|\cdot\|$ the ℓ_2 -norm on \mathbb{R}^n . The power α is unusual, but the role it plays is to flatten out the posterior, effectively discounting the data slightly. Martin et al. (2017) describe this as a regularization that prevents the posterior from chasing the data too closely, and similar discounting ideas have been used for robustness purposes in certain misspecified models (e.g., Grünwald and van Ommen 2017; Holmes and Walker 2017; Syring and Martin 2017). In our present context, the α discount is a technical device to help the posterior adapt to the unknown sparsity (see Martin and Walker 2017) and there are some potential benefits to this discounting when it comes to uncertainty quantification (see Martin and Ning 2018 and Section 3.2 below). In any case, we recommend taking $\alpha \approx 1$ in applications so there is no practical difference between our proposal and a closer-to-genuine Bayes posterior with $\alpha = 1$. In particular, we take $\alpha = 0.99$ in all of our numerical examples. The end result is a posterior distribution, Π^n , for β that depends on α , γ , and, in this case, the known σ^2 .

Importantly, the posterior Π^n is actually relatively easy to understand and compute. Indeed, the conditional posterior distribution for β_S , given S , is just

$$\pi^n(\beta_S \mid S) = \mathbf{N}_{|S|}(\beta_S \mid \hat{\beta}_S, \frac{\sigma^2}{\alpha + \gamma} (X_S^\top X_S)^{-1}). \quad (5)$$

For variable selection-related tasks, the marginal posterior for the configuration, S , is the relevant object, and a closed-form expression is available:

$$\pi^n(S) \propto \pi(S) \left(\frac{\gamma}{\alpha + \gamma}\right)^{|S|/2} \exp\{-\frac{\alpha}{2\sigma^2} \|y - \hat{y}_S\|^2\}, \quad (6)$$

where \hat{y}_S is the fitted response based on the least squares fit to (y, X_S) . From this, one can immediately construct a Metropolis–Hastings procedure to sample S from the posterior π^n ; a shotgun stochastic search strategy could also be taken, as in Liu et al. (2018). If samples from the posterior of β are also desired, then the S sampler can be augmented by sampling from the conditional posterior for β_S , given S , along the way. Contrary to popular belief, posterior sampling of S is *not* prohibitively slow; see Section 4.

2.2 Unknown σ^2

For the realistic case where the error variance is unknown, there are different strategies one can employ. The simplest strategy, taken in Martin et al. (2017), is to construct an estimator, $\hat{\sigma}^2$, and plug it in to the known- σ^2 formulas above. They used a lasso-driven estimator, discussed in Reid et al. (2014), in their numerical examples, and their method had very good performance. But variance estimates post-selection can be unreliable (e.g., Hong et al. 2018), which can impact other posterior summaries, such as credible regions, so we want to consider an alternative based on a prior distribution for σ^2 .

Consider an inverse gamma prior for σ^2 , with density

$$\pi(\sigma^2) = b_0^{a_0} \Gamma(a_0)^{-1} (\sigma^2)^{-(a_0+1)} e^{-b_0/\sigma^2}, \quad \sigma^2 > 0,$$

where a_0 and b_0 are fixed shape and scale parameters, respectively. Incorporating this into the prior formulation described above, expanding the likelihood in (4) as

$$L_n(\beta, \sigma^2) = \mathbf{N}_n(\mathbf{y} \mid X\beta, \sigma^2 I) \propto (\sigma^2)^{-1/2} \exp\left\{-\frac{1}{2\sigma^2} \|\mathbf{y} - X\beta\|^2\right\},$$

to include σ^2 , and combining the two as before, the following properties of the posterior distribution are easy to verify. First, the conditional posterior for β_S , given S and σ^2 is exactly as in (5); second, the conditional posterior distribution for σ^2 , given S , is again inverse gamma with shape = $a_0 + \frac{\alpha n}{2}$ and scale = $b_0 + \frac{\alpha}{2} \|\mathbf{y} - \hat{\mathbf{y}}_S\|^2$; and, finally, the marginal posterior for S is

$$\pi^n(S) \propto \pi(S) \left(\frac{\gamma}{\alpha + \gamma}\right)^{|S|/2} \left\{b_0 + \frac{\alpha}{2} \|\mathbf{y} - \hat{\mathbf{y}}_S\|^2\right\}^{-(a_0 + \alpha n/2)}.$$

Therefore, the MCMC strategy described above to evaluate the posterior can proceed with only simple changes. A Metropolis–Hastings sampler for S can be constructed using this alternative formula for $\pi^n(S)$, and, if desired, samples of (β_S, σ^2) from their conditional posterior distribution, given S , can be readily obtained along the way.

3 Empirical Bayes predictive distribution

3.1 Definition and computation

Given the empirical Bayes posterior defined above, either for known or unknown σ^2 , we can immediately obtain a corresponding predictive distribution. Consider a pair $(\tilde{X}, \tilde{\mathbf{y}})$ where $\tilde{X} \in \mathbb{R}^{d \times p}$ is a given matrix of explanatory variable values at which we seek to predict the corresponding response $\tilde{\mathbf{y}} \in \mathbb{R}^d$.

If σ^2 were known, or if a plug-in estimator is used, then the conditional posterior predictive distribution of $\tilde{\mathbf{y}}$, given S , is familiar, and given by

$$f_{\tilde{X}}^n(\tilde{\mathbf{y}} \mid S) = \mathbf{N}_d(\tilde{\mathbf{y}} \mid \tilde{X}_S \hat{\beta}_S, \sigma^2 I_d + \frac{\sigma^2}{\alpha + \gamma} \tilde{X}_S^\top (X_S^\top X_S)^{-1} \tilde{X}_S).$$

To obtain the predictive distribution for $\tilde{\mathbf{y}}$, we simply need to integrate out S with respect to its posterior, i.e.,

$$f_{\tilde{X}}^n(\tilde{\mathbf{y}}) = \sum_S \pi^n(S) f_{\tilde{X}}^n(\tilde{\mathbf{y}} \mid S). \quad (7)$$

Of course, one cannot evaluate this sum because there are too many terms. However, we can run our previously described MCMC procedure to sample from the posterior distribution of S , resulting in a Monte Carlo approximation of the predictive density $f_{\tilde{X}}^n(\tilde{y})$ at some set values of \tilde{y} . Alternatively, one can sample new \tilde{y} from $f_{\tilde{X}}^n(\tilde{y} | S)$ along the Markov chain. Having a sample from the predictive distribution is advantageous when it comes to creating posterior credible sets for prediction. For example, in the $d = 1$ case, a 95% posterior prediction interval can be found by computing quantiles of the sample taken from the predictive distribution.

Very little changes when the inverse gamma prior for σ^2 is adopted. Indeed, the predictive density $f_{\tilde{X}}^n(\tilde{y} | S)$ is just the density for a d -variate Student-t distribution, with $2a_0 + \alpha n$ degrees of freedom, location $\tilde{X}_S \hat{\beta}_S$, and scale matrix

$$\frac{b_0 + (\alpha/2) \|y - \hat{y}_S\|^2}{a_0 + \alpha n/2} \left(I_d + \frac{1}{\alpha + \gamma} \tilde{X}_S^\top (X_S^\top X_S)^{-1} \tilde{X}_S \right).$$

From here, sampling from the predictive (7) can proceed exactly like before, with straightforward modifications to accommodate the Student-t instead of normal shape.

3.2 Asymptotic properties

The goal here is to explore the theoretical properties of the empirical Bayes predictive distribution defined above. While the computation of this predictive is simple and fast, the somewhat unusual form of the prior and posterior makes it unclear whether this predictive can be useful in any way, so this theoretical analysis is essential. Here we bound the rate at which the posterior concentrates on β vectors that lead to quality prediction of a new observation which, in certain cases, despite the high dimensionality, is close to the parametric root- n rate. We also investigate distributional approximations of the predictive distribution and corresponding uncertainty quantification properties. For simplicity, we focus on univariate prediction, $d = 1$, so the \tilde{X} matrix can be replaced by a p -vector x ; we drop the tilde accent to simplify the notation. Moreover, as is typically done in theoretical analyses of the $p \gg n$ problem (e.g., Castillo et al. 2015), we work in the case of known error variance. Also assume, for simplicity, that the rank of X is n .

To start, for a given $x \in \mathbb{R}^p$ and particular values β and β^* , let $h_x(\beta^*, \beta)$ denote the conditional Hellinger distance between $N(x^\top \beta, \sigma^2)$ and $N(x^\top \beta^*, \sigma^2)$. Following Guhaniyogi and Dunson (2015), define an unconditional Hellinger distance

$$h(\beta^*, \beta) = \left\{ \int h_x^2(\beta^*, \beta) Q_n(dx) \right\}^{1/2},$$

where Q_n is the empirical distribution corresponding to the observed covariate values, i.e., the rows of X . Then the following theorem establishes the posterior concentration rate relative to the prediction-focused metric $h(\beta^*, \beta)$.

Theorem 1. *Let s^* be a sequence with $s^* = o(n)$. Then for the empirical Bayes posterior distribution Π^n as defined above, there exists a constant $M > 0$ such that*

$$\sup_{\beta^*: |S_{\beta^*}| = s^*} \mathbf{E}_{\beta^*} \Pi_n(\{\beta \in \mathbb{R}^p : h(\beta^*, \beta) > M\varepsilon_n\}) \rightarrow 0,$$

where $\varepsilon_n^2 = n^{-1} s^* \log(p/s^*)$.

Proof. Without loss of generality, assume $\sigma^2 = 1$. Let $k_x(\beta^*, \beta)$ denote the conditional Kullback–Leibler divergence of $\mathbf{N}(x^\top \beta, \sigma^2)$ from $\mathbf{N}(x^\top \beta^*, \sigma^2)$. Then we have

$$h_x^2(\beta^*, \beta) \leq 2 k_x(\beta^*, \beta) = |x^\top (\beta - \beta^*)|^2.$$

From the above inequality, upon taking expectation over $x \sim Q_n$, we get

$$h^2(\beta^*, \beta) \leq n^{-1} \|X(\beta - \beta^*)\|^2.$$

Therefore,

$$\{\beta : h^2(\beta^*, \beta) > M^2 n^{-1} s^* \log(p/s^*)\} \subseteq \{\beta : \|X(\beta - \beta^*)\|^2 > M^2 s^* \log(p/s^*)\},$$

and it follows from Theorem 1 in Martin et al. (2017) that, for suitable M , the expected value of the empirical Bayes posterior probability assigned to the right-most set above vanishes uniformly in s^* -sparse β^* , which completes the proof. \square

The conditions here are different from those in Jiang (2007) and Guhaniyogi and Dunson (2015), but it may help to compare the rates obtained. Note that, beyond sparsity, no assumptions are made in Theorem 1 above on the magnitude of β^* , whereas the latter two papers assume $\|\beta^*\|_1 = O(1)$ which requires either (a) s^* grows slowly and non-zero signals vanish slowly, or (b) s^* grows not-so-slowly and the non-zero signals vanish rapidly. The more realistic case is (a), so suppose $s^* \asymp (\log n)^k$ for some $k > 0$. If p is polynomial in n , i.e., $p \asymp n^K$ for any $K > 0$, then we have

$$\varepsilon_n \asymp n^{-1/2} (\log n)^{(k+1)/2},$$

which is nearly the parametric root- n rate. And if p is sub-exponential in n , i.e., if $\log p \asymp n^r$ for $r \in (0, 1)$, then ε_n is $n^{-(1-r)/2}$ modulo logarithmic terms which, again, is close to the parametric rate when r is small. In any case, if the analogy between the sparse normal means problem and the regression problem considered here holds up in the context of prediction, the minimax rate results in Mukherjee and Johnstone (2015) suggest that we cannot improve on the rate ε_n identified in Theorem 1. Of course, the familiar “ $s^* \log(p/s^*)$ ” posterior concentration rate in terms of $\|X(\beta - \beta^*)\|$ has been established for other models, such as horseshoe (e.g., Ghosh and Chakrabarti 2015; van der Pas et al. 2017a, 2014), so the result in Theorem 1 would apply for these models as well.

The next result will connect the convergence rate in Theorem 1 above to the posterior predictive density $f_x^n(\tilde{y})$ defined above. The key to this derivation is convexity of the squared Hellinger distance and the fact that $f_x^n(\tilde{y}) = \int \mathbf{N}(\tilde{y} | x^\top \beta, \sigma^2) \Pi^n(d\beta)$.

Theorem 2. *Let $f_x^*(\tilde{y}) = \mathbf{N}(\tilde{y} | x^\top \beta^*, \sigma^2)$ denote the true distribution of the new observation, for a given x , and let $H(f_x^*, f_x^n)$ denote the Hellinger distance between this and the predictive density f_x^n in (7). Then under the conditions of Theorem 1,*

$$\mathbf{E}_{\beta^*} \int H^2(f_x^*, f_x^n) Q_n(dx) \lesssim \varepsilon_n^2.$$

Proof. Convexity of H^2 , Jensen’s inequality, and Fubini’s theorem gives

$$\begin{aligned} \int H^2(f_x^*, f_x^n) Q_n(dx) &\leq \int \int h_x^2(\beta^*, \beta) \Pi^n(d\beta) Q_n(dx) \\ &= \int h^2(\beta^*, \beta) \Pi^n(d\beta). \end{aligned}$$

For M as in Theorem 1, if we define the set

$$A_n = \{\beta : h(\beta^*, \beta) > M\varepsilon_n\},$$

then the right-hand side above equals

$$\int_{A_n} h^2(\beta^*, \beta) \Pi^n(d\beta) + \int_{A_n^c} h^2(\beta^*, \beta) \Pi^n(d\beta). \quad (8)$$

The first term is bounded by a constant times ε_n^2 by definition of A_n . And since Hellinger distance is no more than 2, the second term is bounded by a constant times $\Pi^n(A_n^c)$. Theorem 1 above shows that $\Pi^n(A_n^c) \rightarrow 0$ in expectation, but the proof of Theorem 1 in Martin et al. (2017) actually gives a bound on that expectation which is $e^{-Gn\varepsilon_n^2}$ for some $G > 0$. Then the claim follows since both terms in (8) are of order ε_n^2 or smaller. \square

As discussed above, in certain cases, this prediction error rate could be arbitrarily close to the parametric root- n rate. The particular metric in Theorem 2 measures the prediction quality for new x 's which are already in the current sample, in other words, it measures in-sample prediction quality. Intuitively, however, we expect that similar conclusions could be made for out-of-sample prediction, provided that the new observation does not differ too much from what we have seen in the data. Indeed, in our simulation experiments, the new x is an independent sample from the distribution that generated the original X , and the prediction accuracy results confirm our intuition. In any case, we teach our students that extrapolation—predicting outside the range of the given data—is dangerous, so this type of “near-sample” prediction is most relevant.

Beyond prediction accuracy, one would also want the posterior predictive distribution to be calibrated in the sense that a $100(1 - \zeta)\%$ prediction interval, for $\zeta \in (0, \frac{1}{2})$, has coverage probability $1 - \zeta$, at least approximately. That is, one may ask if the predictive distribution above provides valid uncertainty quantification. To first build some intuition, recall the predictive density in (7):

$$f_x^n(\tilde{y}) = \sum_S \pi^n(S) \mathbf{N}(\tilde{y} \mid x^\top \hat{\beta}_S, \sigma^2 + \frac{\sigma^2}{\alpha + \gamma} x_S^\top (X_S^\top X_S)^{-1} x_S).$$

Theorems 4–5¹ in Martin et al. (2017) investigate the posterior distribution for S and, in particular, give conditions under which $\mathbb{E}_{\beta^*} \pi^n(S^*) \rightarrow 1$. In such cases, we have

$$f_x^n(\tilde{y}) \approx \mathbf{N}(\tilde{y} \mid x^\top \hat{\beta}_{S^*}, \sigma^2 + \frac{\sigma^2}{\alpha + \gamma} x_{S^*}^\top (X_{S^*}^\top X_{S^*})^{-1} x_{S^*}),$$

and one will recognize the right-hand side as roughly the *oracle* predictive distribution, the one based on knowledge of the correct configuration S^* . The only difference between this predictive distribution and the standard fixed-model version found in textbooks is the factor $(\alpha + \gamma)^{-1}$. We prefer our predictive density to be at least as wide as the oracle, which suggests choosing (α, γ) such that $\alpha + \gamma \leq 1$, maybe strictly less than 1. With this choice, we would expect the posterior prediction intervals to be approximately calibrated in terms of frequentist coverage probability, and our numerical results in Section 4 confirm

¹There are some minor mistakes in the statement and proof of Theorem 5 in Martin et al. (2017), but see the supplement at <https://arxiv.org/abs/1406.7718> for corrections.

this expectation, for both the known- and unknown- σ^2 cases. In our examples we also observe similarly good coverage for prediction intervals derived from the model that starts with the horseshoe prior, which is expected based on the theoretical results in van der Pas et al. (2017b) for the normal means model.

To make the above heuristics precise, write the posterior distribution for β as

$$\Pi^n(B) = \sum_S \pi^n(S) \{ \mathbf{N}_{|S|}(\hat{\beta}_S, \frac{\sigma^2}{\alpha+\gamma}(X_S^\top X_S)^{-1}) \otimes \delta_{0_{S^c}} \}(B), \quad B \subseteq \mathbb{R}^p.$$

For the given $x \in \mathbb{R}^p$, set $\psi = x^\top \beta$. Then the derived posterior distribution for ψ is

$$\Pi_\psi^n(A) := \sum_S \pi^n(S) \mathbf{N}(A \mid \hat{\psi}_S, \sigma^2 v_S), \quad A \subseteq \mathbb{R},$$

where $\hat{\psi}_S = x_S^\top \hat{\beta}_S$ and $v_S = \frac{1}{\alpha+\gamma} x_S^\top (X_S^\top X_S)^{-1} x_S$. Then we have the following Bernstein–von Mises theorem, similar to that in Martin and Ning (2018), which almost immediately implies that the posterior predictive distribution provides valid uncertainty quantification.

Theorem 3. Write $d_{\text{TV}}(P, Q) = \sup_A |P(A) - Q(A)|$ for the total variation distance between probability measures P and Q . Let $\mathbf{N}(\hat{\psi}_{S^*}, \sigma^2 v_{S^*})$ denote the oracle posterior for ψ based on knowledge of the true configuration S^* . If $\mathbb{E}_{\beta^*} \pi^n(S^*) \rightarrow 1$, then

$$\mathbb{E}_{\beta^*} d_{\text{TV}}(\Pi_\psi^n, \mathbf{N}(\hat{\psi}_{S^*}, \sigma^2 v_{S^*})) \rightarrow 0.$$

Proof. Define $D_n(A) = |\Pi_\psi^n(A) - \mathbf{N}(A \mid \hat{\psi}_{S^*}, \sigma^2 v_{S^*})|$ for Borel sets $A \subseteq \mathbb{R}$. Since $|\sum_i a_i| \leq \sum_i |a_i|$, we immediately get the following upper bound:

$$D_n(A) \leq \sum_S \pi^n(S) |\mathbf{N}(A \mid \hat{\psi}_S, \sigma^2 v_S) - \mathbf{N}(A \mid \hat{\psi}_{S^*}, \sigma^2 v_{S^*})|.$$

The absolute difference above is 0 when $S = S^*$ and bounded by 2 otherwise, so

$$d_{\text{TV}}(\Pi_\psi^n, \mathbf{N}(\hat{\psi}_{S^*}, \sigma^2 v_{S^*})) \leq 2 \sum_{S \neq S^*} \pi^n(S) = 2\{1 - \pi^n(S^*)\}.$$

After taking expectation of both sides, the upper bound vanishes by assumption. \square

Corollary 1. If $\mathbb{E}_{\beta^*} \pi^n(S^*) \rightarrow 1$, then $\mathbb{E}_{\beta^*} d_{\text{TV}}(f_x^n, \mathbf{N}(\hat{\psi}_{S^*}, \sigma^2(1 + v_{S^*}))) \rightarrow 0$.

Proof. The predictive distribution is a convolution of the posterior Π_ψ^n with $\mathbf{N}(0, \sigma^2)$ and, similarly, the oracle predictive is a convolution of $\mathbf{N}(\hat{\psi}_{S^*}, \sigma^2 v_{S^*})$ with $\mathbf{N}(0, \sigma^2)$. So the result follows from general results on information loss, e.g., Lemma B.11 and Equation (B.14) in Ghosal and van der Vaart (2017). \square

The conclusion of Corollary 1 is that the predictive distribution will closely resemble the oracle predictive distribution based on knowledge of S^* . To visualize this, Figure 1 shows a sample from our posterior predictive distribution with the oracle predictive density function overlaid, for the case with $n = 200$ and $p = 300$. In fact, these computations were done under the unknown- σ^2 scenario, so that the oracle is a shifted and scaled Student-t density. That the two distributions match very closely confirms Corollary 1,

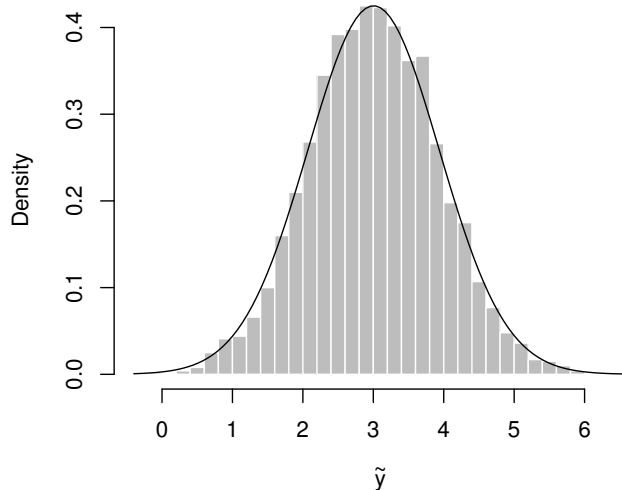


Figure 1: Histogram of a Monte Carlo sample drawn from the posterior predictive distribution, f_x^n , and the corresponding oracle predictive density function overlaid.

but it is perhaps surprising that the accuracy of the normal approximation kicks in with only $n = 200$, even for a relatively high-dimensional setting.

From the above Bernstein–von Mises result, which is in terms of a strong, total variation distance, implies that, e.g., 95% posterior prediction intervals derived from f_x^n would look like $\hat{\psi}_{S^*} \pm 1.96 \sigma(1 + v_{S^*})^{1/2}$, which is known to have prediction coverage probability at least 0.95, provided that $\alpha + \gamma \leq 1$. Therefore, if $\alpha + \gamma \leq 1$, then the posterior prediction intervals derived from f_x^n provide valid uncertainty quantification asymptotically.

4 Numerical results

4.1 Methods

We investigate the performance of two versions of the proposed empirical Bayes method: EB1 uses a plug-in estimator of the error variance based on a least squares fit after a preliminary variable selection step based on adaptive lasso; and EB2 uses the inverse gamma prior for σ^2 as described in Section 2.2, with hyperparameters $(a_0, b_0) = (0.01, 4)$. Both EB1 and EB2 use the following hyperparameter settings: $\alpha = 0.99$, $\gamma = 0.005$, $a = 0.05$, and $c = 1$. R code to implement EB1 and EB2 is available at <https://www4.stat.ncsu.edu/~rmartin/research.html>. These are compared to predictions based on two versions of the horseshoe: the first, denoted by HS1, uses the same plug-in estimator of the error variance as EB1; the second, denoted by HS2, uses the default Jeffreys prior for σ^2 implemented in the `horseshoe` package (van der Pas et al. 2016). The aforementioned methods give full predictive distributions, which yield both point predictions and prediction intervals. We also compare with point predictions obtained from lasso and adaptive lasso using the R packages `lars` and `parcor`, respectively.

p		$A = 2$			$A = 4$			$A = 8$		
		$r = 0.2$	0.5	0.8	$r = 0.2$	0.5	0.8	$r = 0.2$	0.5	0.8
125	EB1	0.86	1.13	0.99	1.15	0.91	0.94	0.98	0.99	1.22
	EB2	0.86	1.13	0.99	1.15	0.91	0.94	0.98	0.99	1.22
	HS1	0.87	1.18	1.06	1.18	0.98	1.03	1.01	1.04	1.30
	HS2	0.89	1.21	1.07	1.20	1.01	1.05	1.03	1.07	1.31
	Lasso	1.18	1.51	1.38	1.57	1.48	1.48	1.66	1.51	1.90
	Alasso	0.93	1.15	1.05	1.70	1.45	1.76	5.20	3.53	8.99
250	EB1	1.05	1.10	1.12	1.07	1.24	0.87	1.15	1.07	0.96
	EB2	1.05	1.10	1.12	1.07	1.24	0.87	1.15	1.07	0.96
	HS1	1.08	1.13	1.16	1.08	1.31	0.94	1.17	1.08	0.98
	HS2	1.12	1.19	1.17	1.12	1.34	0.98	1.20	1.12	1.00
	Lasso	1.31	1.50	1.52	1.38	1.69	1.35	1.31	1.35	1.33
	Alasso	1.07	1.14	1.23	1.50	1.92	2.07	3.47	4.14	5.60
500	EB1	0.97	0.93	0.94	0.93	1.16	1.08	1.01	1.02	1.17
	EB2	0.97	0.93	0.93	0.93	1.16	1.08	1.01	1.02	1.17
	HS1	0.98	0.98	0.97	0.96	1.16	1.04	1.01	1.04	1.17
	HS2	1.00	1.08	0.99	1.09	1.15	1.05	1.12	1.04	1.19
	Lasso	1.28	1.37	1.44	1.49	1.35	1.25	1.43	1.55	1.44
	Alasso	0.98	1.00	1.12	1.35	1.44	2.14	4.54	3.83	6.52

Table 1: Comparison of mean square prediction error (MSPE) for the six different methods across various settings—of dimension $p \in \{125, 250, 500\}$, signal size $A \in \{2, 4, 8\}$, and correlation $r \in \{0.2, 0.5, 0.8\}$ —as described in the text.

4.2 Simulated data experiments

We are mainly interested in the moderate p setting, with n smaller than p and p less than or equal to 500, which is common in medical and social science applications. We look at both the prediction error and the coverage rates and length of prediction intervals produced by the proposed method compared to the above competitors.

We selected five specific β_j 's to be non-zero, with the rest being zero. Our signal configuration places the signals at positions 3, 4, 15, 22, and 25 in the p -vector β . This configuration captures a number of different features, including a pair of signals that are together, i.e., 3 and 4, a large gap between 4 and 15, and a pair that is relatively close together, i.e., 22 and 25. All of the non-zero β_j 's take value A , where $A \in \{2, 4, 8\}$. Finally, the rows of the design matrix, X , are p -variate normal with zero mean, unit variance, and first-order autoregressive dependence structure, with correlation parameter $r \in \{0.2, 0.5, 0.8\}$. For each (A, r) pair, we use $n = 100$, and $p \in \{125, 250, 500\}$. This yields a total of 27 different simulation settings. For each setting, we compare results from 250 runs. The choice of 250 allows us to evaluate the coverage accuracy of the 95% prediction intervals. The point prediction comparisons, in terms of mean square prediction error (MSPE) are shown in Table 1, and the prediction interval coverage probabilities and mean lengths are presented in Tables 2 and 3, respectively.

Both EB1 and EB2 perform very well across all the settings in terms of MSPE, with HS1 and HS2 performing similarly, and all four of these generally beating lasso and

p		$A = 2$			$A = 4$			$A = 8$		
		$r = 0.2$	0.5	0.8	$r = 0.2$	0.5	0.8	$r = 0.2$	0.5	0.8
125	EB1	0.96	0.94	0.95	0.96	0.97	0.96	0.98	0.99	0.97
	EB2	0.96	0.94	0.96	0.95	0.96	0.97	0.97	0.96	0.94
	HS1	0.98	0.95	0.96	0.96	0.97	0.96	0.98	0.97	0.94
	HS2	0.96	0.92	0.96	0.93	0.96	0.94	0.96	0.94	0.92
250	EB1	0.95	0.95	0.95	0.96	0.96	0.98	0.98	0.98	0.99
	EB2	0.95	0.96	0.95	0.96	0.94	0.96	0.94	0.96	0.95
	HS1	0.96	0.97	0.96	0.98	0.96	0.96	0.95	0.95	0.97
	HS2	0.95	0.96	0.94	0.96	0.92	0.96	0.94	0.94	0.95
500	EB1	0.95	0.96	0.96	0.98	0.96	0.98	0.98	0.98	0.98
	EB2	0.95	0.95	0.96	0.96	0.94	0.96	0.96	0.93	0.94
	HS1	0.96	0.96	0.97	0.98	0.97	0.96	0.97	0.95	0.94
	HS2	0.95	0.94	0.95	0.93	0.94	0.96	0.95	0.92	0.93

Table 2: Comparison of coverage probability for the four different 95% prediction intervals across various settings—of dimension $p \in \{125, 250, 500\}$, signal size $A \in \{2, 4, 8\}$, and correlation $r \in \{0.2, 0.5, 0.8\}$ —as described in the text.

adaptive lasso. Our empirical Bayes methods are based on a two-groups or spike-and-slab model formulation, which are believed to be difficult and more expensive to compute. However, contrary to this popular belief, EB1 and EB2 take only about 20% of the time required to compute the horseshoe predictions using the R package, which confirms the claim made in Martin and Ning (2018) in a different context.

For the 95% prediction interval comparisons, we investigate the coverage probability and mean length for two empirical Bayes methods, the two horseshoe methods, and an *oracle* predictive distribution that knows the true configuration S^* . Here we sample a new pair (\tilde{x}, \tilde{y}) from the true model and construct prediction intervals for \tilde{y} with \tilde{x} as the input. Of course, the coverage probabilities for the oracle prediction interval are exactly 0.95, but, according to Table 2, the other four methods all generally have prediction coverage probability within an acceptable range of the target level. And in terms of interval lengths, Table 3 reveals that all four methods are comparable in efficiency to the oracle prediction intervals. This confirms the claims made based on the theoretical results in Section 3.2. Note, however, that the “version 2” of both methods tends to perform better, since the plug-in estimation of the error variance is rather unstable.

The take-away message here is that the two empirical Bayes methods, in particular, EB2, based on the prior for the error variance, is as good or better than the horseshoe-based methods across a range of settings, in terms of both prediction accuracy and uncertainty quantification. On top of its strong statistical performance, our EB2 method is more efficient computationally, as it generally finishes 5 times faster than the implementation of horseshoe in the corresponding R package.

p		$A = 2$			$A = 4$			$A = 8$		
		$r = 0.2$	0.5	0.8	$r = 0.2$	0.5	0.8	$r = 0.2$	0.5	0.8
125	EB1	4.02	4.04	4.11	4.68	4.66	5.19	7.52	7.43	8.76
	EB2	4.12	4.13	4.15	4.11	4.14	4.16	4.13	4.10	4.17
	HS1	4.43	4.41	4.34	4.43	4.42	4.33	4.43	4.41	4.35
	HS2	4.15	4.16	4.17	4.15	4.18	4.16	4.15	4.13	4.16
	Oracle	4.06	4.07	4.07	4.05	4.09	4.08	4.07	4.04	4.07
250	EB1	4.04	4.07	4.19	4.59	4.71	5.44	6.76	7.57	8.27
	EB2	4.13	4.15	4.18	4.12	4.14	4.13	4.15	4.12	4.14
	HS1	4.43	4.41	4.37	4.44	4.42	4.34	4.44	4.41	4.35
	HS2	4.14	4.17	4.15	4.13	4.14	4.09	4.16	4.12	4.12
	Oracle	4.07	4.09	4.09	4.06	4.08	4.05	4.09	4.07	4.05
500	EB1	4.05	4.07	4.22	4.75	4.79	5.38	7.42	7.09	8.57
	EB2	4.12	4.14	4.17	4.08	4.15	4.15	4.10	4.12	4.18
	HS1	4.32	4.31	4.27	4.31	4.32	4.27	4.32	4.32	4.28
	HS2	4.10	4.08	4.11	4.05	4.09	4.07	4.05	4.09	4.10
	Oracle	4.07	4.08	4.08	4.04	4.08	4.05	4.04	4.06	4.09

Table 3: Comparison of mean length for the five different 95% prediction intervals across various settings—of dimension $p \in \{125, 250, 500\}$, signal size $A \in \{2, 4, 8\}$, and correlation $r \in \{0.2, 0.5, 0.8\}$ —as described in the text.

4.3 Real data application

Following the example used in Bhadra et al. (2017), we use the same real-world data set to examine how our method performs. This pharmacogenomics data set is publicly available in the NCI-60 database, and can be accessed via the R package `mixOmics` and dataset `multidrug`. The expression level of 12 different human ABC transporter genes are predicted using compound concentration levels. To keep our analysis on par with that in Bhadra et al. (2017), we only predict with the 853 compounds that have no missing values. The data set includes 60 samples, which we randomly split into a train and test set of 75% and 25%, respectively. Thus, in this regression scenario, $n = 45$ and $p = 853$. Each random train and test split is performed 20 times, and we calculate the average out-of-sample MSPE for these 20 trials, shown in Table 4.

For the 12 different transporter genes, our empirical Bayes method obtained better average out-of-sample MSPE in three of the genes (A2, A8, and A12) than those from the other methods implemented, while being very comparable with the other methods on the other 9 genes as response variables. The take-away message, again, is that the empirical Bayes method is as good or better than horseshoe or lasso-based methods in terms of prediction quality, provides accurate predictive uncertainty quantification, and with lower computational cost than the horseshoe.

Response	EB1	EB2	HS1	HS2	Lasso	Alasso
A1	0.95	0.93	1.02	0.93	0.97	1.00
A2	0.94	0.93	0.97	0.94	1.09	0.99
A3	1.03	0.93	1.02	0.93	0.97	1.07
A4	0.97	0.93	0.98	0.93	0.88	1.00
A5	0.93	0.93	0.93	0.96	0.92	0.94
A6	0.93	0.93	0.93	0.93	0.98	0.93
A7	0.93	0.93	0.94	0.93	1.07	0.92
A8	0.93	0.93	0.94	0.94	1.06	1.01
A9	0.97	0.93	0.99	0.92	0.82	0.92
A10	0.93	0.93	0.93	0.93	0.99	0.93
A12	1.00	0.93	1.00	0.95	1.04	1.04
B1	0.72	0.73	0.58	0.54	0.61	0.42

Table 4: Mean square prediction error for the five methods averaged over 20 random training/testing splits of the data as described in Section 4.3. The rows correspond to different response variables being predicted.

5 Discussion

In this paper, we apply a recently proposed empirical Bayes method to the context of prediction in sparse high-dimensional linear regression settings. The key idea is to let the data inform the prior center so that the tail of the prior distribution have little influence on the posterior concentration properties. This allows for faster computation—since conjugate Gaussian priors can be used for the non-zero regression coefficients—without sacrificing on posterior concentration rates. In the context of prediction, being able to formulate the Bayesian model using conjugate priors means that the predictive distribution can be written (almost) in closed-form; it allows for some analytical integration, yielding a relatively easy to compute posterior predictive distribution for the purpose of constructing prediction intervals, etc. We also extended the theoretical results presented in Martin et al. (2017) to obtain posterior concentration rates relevant to the prediction problem and establishing a Bernstein–von Mises theorem the sheds light on the empirical Bayes posterior’s potential for valid uncertainty quantification in prediction. All these desirable features are confirmed by the results in real- and simulated-data examples.

An interesting question is if this empirical Bayes methodology can be extended to handle sparse, high-dimensional generalized linear models, such as logistic regression. In the Gaussian setting considered here, the notion of prior centering is quite natural and relatively simple to arrange, but the idea itself is not specific to Gaussian models. Work is underway to carry out this non-trivial extension, and we expect that similarly good theoretical and numerical results, like those obtained here for prediction, can be established in that more general context too.

Acknowledgment

This work is partially supported by the National Science Foundation, DMS–1737933.

References

- Bhadra, A., Datta, J., Li, Y., Polson, N., and Willard, B. (2017). Prediction risk for the horseshoe regression. Unpublished manuscript, [arXiv:1605.04796](#).
- Bhattacharya, A., Pati, D., Pillai, N. S., and Dunson, D. B. (2015). Dirichlet-Laplace priors for optimal shrinkage. *J. Amer. Statist. Assoc.*, 110(512):1479–1490.
- Carvalho, C. M., Polson, N. G., and Scott, J. G. (2010). The horseshoe estimator for sparse signals. *Biometrika*, 97(2):465–480.
- Castillo, I., Schmidt-Hieber, J., and van der Vaart, A. (2015). Bayesian linear regression with sparse priors. *Ann. Statist.*, 43(5):1986–2018.
- Fan, J. and Li, R. (2001). Variable selection via nonconcave penalized likelihood and its oracle properties. *J. Amer. Statist. Assoc.*, 96(456):1348–1360.
- Ghosal, S. and van der Vaart, A. (2017). *Fundamentals of Nonparametric Bayesian Inference*, volume 44 of *Cambridge Series in Statistical and Probabilistic Mathematics*. Cambridge University Press, Cambridge.
- Ghosh, P. and Chakrabarti, A. (2015). Posterior concentration properties of a general class of shrinkage estimators around nearly black vectors. Unpublished manuscript, [arXiv:1412.8161](#).
- Grünwald, P. and van Ommen, T. (2017). Inconsistency of Bayesian inference for misspecified linear models, and a proposal for repairing it. *Bayesian Anal.*, 12(4):1069–1103.
- Guhaniyogi, R. and Dunson, D. B. (2015). Bayesian compressed regression. *J. Amer. Statist. Assoc.*, 110(512):1500–1514.
- Holmes, C. C. and Walker, S. G. (2017). Assigning a value to a power likelihood in a general Bayesian model. *Biometrika*, 104(2):497–503.
- Hong, L., Kuffner, T. A., and Martin, R. (2018). On overfitting and post-selection uncertainty assessments. *Biometrika*, 105(1):221–224.
- Jiang, W. (2007). Bayesian variable selection for high dimensional generalized linear models: convergence rates of the fitted densities. *Ann. Statist.*, 35(4):1487–1511.
- Leeb, H. (2006). The distribution of a linear predictor after model selection: unconditional finite-sample distributions and asymptotic approximations. In *Optimality*, volume 49 of *IMS Lecture Notes Monogr. Ser.*, pages 291–311. Inst. Math. Statist., Beachwood, OH.
- Leeb, H. (2009). Conditional predictive inference post model selection. *Ann. Statist.*, 37(5B):2838–2876.
- Liu, C., Yang, Y., Bondell, H., and Martin, R. (2018). Bayesian inference in high-dimensional linear models using an empirical correlation-adaptive prior. Unpublished manuscript, [arXiv:1810.00739](#).

- Martin, R., Mess, R., and Walker, S. G. (2017). Empirical Bayes posterior concentration in sparse high-dimensional linear models. *Bernoulli*, 23(3):1822–1847.
- Martin, R. and Ning, B. (2018). Empirical priors and coverage of posterior credible sets in a sparse normal mean model. Unpublished manuscript, [arXiv:1812.02150](#).
- Martin, R. and Walker, S. G. (2014). Asymptotically minimax empirical Bayes estimation of a sparse normal mean vector. *Electron. J. Stat.*, 8(2):2188–2206.
- Martin, R. and Walker, S. G. (2017). Empirical priors for target posterior concentration rates. Unpublished manuscript, [arXiv:1604.05734](#).
- Mukherjee, G. and Johnstone, I. M. (2015). Exact minimax estimation of the predictive density in sparse Gaussian models. *Ann. Statist.*, 43(3):937–961.
- Pötscher, B. M. and Leeb, H. (2009). On the distribution of penalized maximum likelihood estimators: the LASSO, SCAD, and thresholding. *J. Multivariate Anal.*, 100(9):2065–2082.
- Reid, S., Tibshirani, R., and Friedman, J. (2014). A study of error variance estimation in lasso regression. Unpublished manuscript, [arXiv:1311.5274](#).
- Syring, N. and Martin, R. (2017). Calibrating general posterior credible regions. *Biometrika*, to appear, [arXiv:1509.00922](#).
- Tibshirani, R. (1996). Regression shrinkage and selection via the lasso. *J. Roy. Statist. Soc. Ser. B*, 58(1):267–288.
- van der Pas, S., Scott, J., Chakraborty, A., and Bhattacharya, A. (2016). *horseshoe: Implementation of the Horseshoe Prior*. R package version 0.1.0.
- van der Pas, S., Szabó, B., and van der Vaart, A. (2017a). Adaptive posterior contraction rates for the horseshoe. *Electron. J. Stat.*, 11(2):3196–3225.
- van der Pas, S., Szabó, B., and van der Vaart, A. (2017b). Uncertainty quantification for the horseshoe (with discussion). *Bayesian Anal.*, 12(4):1221–1274. With a rejoinder by the authors.
- van der Pas, S. L., Kleijn, B. J. K., and van der Vaart, A. W. (2014). The horseshoe estimator: posterior concentration around nearly black vectors. *Electron. J. Stat.*, 8(2):2585–2618.
- Zellner, A. (1986). On assessing prior distributions and Bayesian regression analysis with g -prior distributions. In *Bayesian Inference and Decision Techniques*, volume 6 of *Stud. Bayesian Econometrics Statist.*, pages 233–243. North-Holland, Amsterdam.
- Zou, H. (2006). The adaptive lasso and its oracle properties. *J. Amer. Statist. Assoc.*, 101(476):1418–1429.